JOURNAL OF APPLIED ELECTROCHEMISTRY 18 (1988) 339–346

High-rate electrochemical copper deposition on bars

L. J. J. JANSSEN

Laboratory for Electrochemistry, Faculty of Chemical Technology, Eindhoven University of Technology, The Netherlands

Received 8 June 1987; revised 29 September 1987

The industrial electrodeposition of copper from cupric acid sulphate baths is typically carried out at approximately $3\,kA\,m^{-2}$. A much higher rate of copper deposition is necessary to improve this electroplating process significantly. To achieve this higher rate for the deposition of copper on a round bar, the solution flow is directed normal to the axis of a round bar. The current efficiency η_{Cu} for copper deposition on a round bar, 9 mm in diameter, has been determined from 1 M H_2SO_4 + 1 M $CuSO_4$ bath as a function of current density, solution flow rate and temperature. A set of relations has been proposed for calculating the current efficiency η_{Cu} for a broad range of parameters.

Nomenclature

A_e working-electrode surface area (m^2)
c_i concentration of a species i ($mol\,m^{-3}$)
c_i^σ c_i at electrode surface ($mol\,m^{-3}$)
c_i^s c_i in bulk of solution ($mol\,m^{-3}$)
D_i diffusion coefficient of a species i ($m^2\,s^{-1}$)
d_c diameter of working electrode (mm)
E electrode potential (V)
E_r reversible electrode potential (V)
F Faraday number, F = $96487\,C\,mol^{-1}$
I current (A)
i current density ($kA\,m^{-2}$, $A\,m^{-2}$)
k_i diffusion mass transfer coefficient for species i ($m\,s^{-1}$)
$k_{f,i}$ k_i with forced convection and without gas-bubble formation ($m\,s^{-1}$)
k_i^e electrochemical rate constant for formation of species i ($m\,s^{-1}$)
K_l equilibrium constant ($mol\,m^{-3}$)
n number of electrons involved in electrode reaction
Q charge
R gas constant, R = $8.31\,J\,K\,mol^{-1}$
Sc Schmidt number: $Sc = v/D$
Sh Sherwood number, $Sh = kd_c/D$
t time (s)
T temperature (K)
Re Reynolds number: $Re = v_c d_c/v$
v flow rate of solution through slots of cell ($m\,s^{-1}$)
v_c flow rate of solution (2.1) ($m\,s^{-1}$)
ϱ density of solution ($kg\,m^{-3}$)
μ dynamic viscosity of solution ($kg\,m^{-1}\,s^{-1}$)
ν kinematic viscosity of solution ($m^2\,s^{-1}$)
η current efficiency

Subscripts
a anodic reaction
c cathodic reaction
D limited by diffusion
f forced convection
L limited by diffusion and migration
N standard

Superscripts
e electrochemical
s bulk of solution
σ surface of working electrode

1. Introduction

In practice, cupric sulphate–sulphuric acid baths are often used to electrodeposit copper on bars. The obtainable deposition rate depends chiefly on the efficiency of agitation of the solution in order to prevent excessive concentration polarization [1]. In industrial copper electrolysis, enhancement of the transfer of cupric ions is mainly achieved by air sparging directly onto the working electrode in the electrolytic cell. In this case, copper deposits of acceptable quality are obtained at current densities of less than about $3\,kA\,m^{-2}$, that is equivalent to $0.42\,mm\,h^{-1}$ [2]. Higher rates of copper deposition are necessary to reduce production costs. In this study, the effect of forced solution flow directed normal to the axes of a round bar on the rate of copper deposition has been investigated. In particular, the effects of the rate of solution flow, the current density and the temperature on the current efficiency for copper deposition from a $CuSO_4$–H_2SO_4 bath have been determined. From these results a set of relations has been proposed to calculate the current efficiency for copper deposition.

2. Experimental details

2.1. *Electrolytic cell and solution circuit*

The electrolytic cell is shown schematically in Fig. 1. The cell consists of two concentric cylinders, each 60 mm in length. The inner cylinder is 20 mm inner and 25 mm outer diameter. The inner diameter of the outer cylinder is 50 mm. The space between the

0021-891X/88 $03.00 + .12

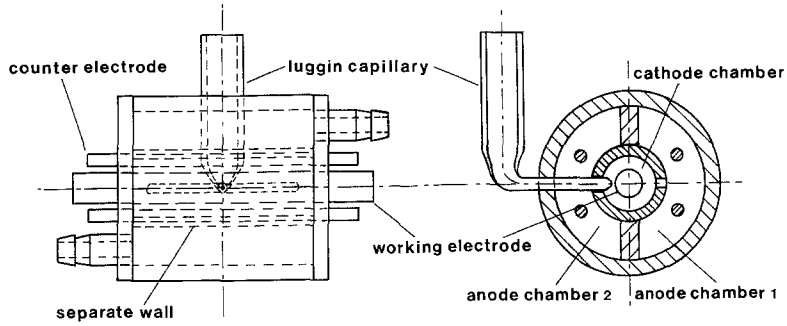

Fig. 1. Scheme of the electrolytic cell.

cylinders is divided into the two equal counter-electrode compartments. The inner cylinder serves as the working-electrode compartment and has two rectangular slots, 60 × 2.7 mm^2 each. Each slot connects the compartment of the working electrode with one counter-electrode compartment. The solution in the cell subsequently flows through a counter-electrode compartment, the working-electrode compartment and the other counter-electrode compartment. The working electrode is a platinum tube 9 mm in outer diameter, 60 mm in length and 17 × 10^{-4} m^2 in electrode surface area. The wall thickness of the platinum tube is 0.25 mm. There is a current connection at each end of the platinum tube.

It was shown that the ohmic potential drop across the platinum tube is negligible even at the highest current (25 A) applied. Four copper rods 3 mm in diameter and 60 mm in length served as the counter electrode; two rods were placed in each counter-electrode compartment. The temperature of the solution was measured in the overflow vessel and maintained at a constant value to within 1° C.

A common solution circuit for forced convection conditions was used. A solution of about 0.01 m^3 was pumped through a circuit consisting of the electrolytic cell, overflow vessel, heat exchanger, pump and flow meters. The flow rate of solution through both rectangular slots was denoted v. The flow rate of solution in the working-electrode compartment at the cross-section, v_c, is equal to the volumetric rate through the cell divided by the difference between the cross-section of the working-electrode compartment and that of the working electrode, both in the direction of the axis of the working electrode.

To visualize the pattern of the solution flow, the cell and the solution circuit were filled with water and a small quantity of blue ink was injected. It was observed that the whole length of both slots was practically uniformly used for solution flow.

2.2. *Electrical measurements and electrolyte*

In this study, a dilute and a concentrated cupric sulphate–sulphuric acid solution, 0.020 M $CuSO_4$ + 1.0 M H_2SO_4 and 1.0 M $CuSO_4$ + 1.0 M H_2SO_4, respectively, were used.

For the current-efficiency measurements the copper deposition took place galvanostatically during a period of 30 s, unless otherwise stated. To verify the effect of time of copper deposition, experiments with a constant quantity of charge were carried out. The potential of the working electrode during copper deposition was recorded as a function of the deposition time, t_c. The charge, Q_c, used during copper deposition is equal to $I_c t_c$.

The quantity of copper deposited on the platinum tube was determined potentiostatically by anodic stripping. The current, I_a, during the anodic stripping was recorded as a function of the stripping time, t_a. The charge, Q_a, used for copper dissolution is given by

$$Q_a = \int_0^{t_a} I_a(t)\mathrm{d}t.$$

The mass transfer coefficient for Cu(II) with forced convection, and both in the absence and presence of gas-bubble evolution, was determined for the dilute solution.

Current-efficiency measurements were used to obtain the mass transfer coefficient for Cu(II) with gas-bubble evolution during copper deposition. To determine the mass transfer coefficient for Cu(II) in the absence of gas-bubble evolution, potential–current curves were measured potentiostatically. A saturated calomel electrode served as the reference electrode and a solution of 0.5 M K_2SO_4 and agar–agar as the salt bridge. The experiment started at a potential of 500 mV and was decreased in steps of 100 mV. The current was determined after waiting for 1 min.

Table 1. Data for the dilute and the concentrated cupric sulphate solution at 323 K

	Dilute solution	*Concentrated solution*
$CuSO_4$ (kmol m^{-3})	0.020	1.0
H_2SO_4 (kmol m^{-3})	1.0	1.0
Viscosity (kg m^{-1} s^{-1})	6.60 × 10^{-4}	8.68 × 10^{-4}
Kinematic viscosity (m^2 s^{-1})	6.30 × 10^{-7}	7.29 × 10^{-7}
Density (kg m^{-3})	1047	1190
Diffusion coefficient $D_{Cu(II)}$ (m^2 s^{-1})	1.06 × 10^{-9}	0.88 × 10^{-9}
Apparent transference number $t_{Cu(II)}$	0.04	0.16
Schmidt number Sc	594	828
Solution flow rate v (m s^{-1})	0.057–1.02	0.040–0.84
Solution flow rate v_c (m s^{-1})	0.013–0.23	0.009–0.19
Reynolds number Re	190–3290	110–2340

3. Results

3.1. *Parameters and dimensionless numbers for cupric sulphate solutions*

Data for the dilute and the concentrated cupric sulphate solution at 323 K are given in Table 1. The viscosity, μ, and the density, ϱ, of the solutions were determined by conventional methods. The diffusion coefficient $D_{Cu(II)}$ in solutions containing H_2SO_4 and $CuSO_4$ and its temperature dependence were calculated using relations 41 and 42 from [3].

Newman [4] has calculated the ratio between the limiting current, I_L, and diffusion-limiting current, I_D, for Cu deposition from solutions at various concentration ratios of $CuSO_4$ to H_2SO_4. The apparent transference number $t_{Cu(II)} = (I_L - I_D)/I_D$ [5]. The Schmidt number $Sc = \nu/D_{Cu(II)}$ and the Reynolds number $Re = v_c d_c/\nu$, where d_c is the diameter of the working-cylinder electrode [6].

3.2. *Cathodic reactions*

Whether the evolution of hydrogen occurs during the deposition of copper depends strongly on the cathodic current density and the rate of solution flow. To obtain insight into the effect of these parameters on cathodic reactions we determined visually whether or not bubble formation occurred at the cathode for the concentrated solution under different electrolytic conditions at 323 K. No hydrogen-bubble formation was visible at 15 kA m^{-2} for $v > 0.21$ m s^{-1} and at 10 kA m^{-2} for $v > 0.13$ m s^{-1}. It should be noted that observation of small bubbles is difficult at high flow rates of the solution. Since the quality of the copper coating obtained under conditions in which hydrogen-bubble formation takes place visibly is poor, the current efficiency for copper was not determined under these conditions. No oxygen was formed during the anodic dissolution of the copper anodes. Consequently, oxygen was not present in the electrolytic cell during copper deposition on the Pt cylinder.

3.3. *Anodic stripping current*

The potentiostatic stripping of copper from the platinum tube electrode yielded I_a/t_a curves whose shape depended on the current density during the cathodic deposition of copper, rate of solution flow and temperature. Characteristic curves at several current densities and at $v = 0.84$ m s^{-1} are given in Fig. 2. The curves for the two highest current densities have two clearly distinguishable waves. The results of Fig. 2 were obtained at an anodic stripping potential of 150 mV. Similar results were found at more positive anodic stripping potentials. The steps in the curves of Fig. 2 may be caused by formation of oxide films during the anodic oxidation of copper.

The I_a/t_a curve at 323 K and 14.7 kA m^{-2} also showed two waves at $v > 0.40$ m s^{-1}, but only one wave at $v < 0.40$ m s^{-1}. The effect of temperature on

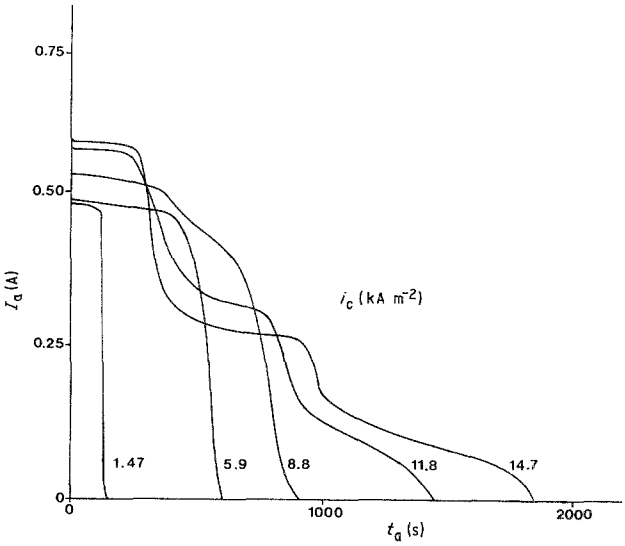

Fig. 2. Anodic current, I_a, as a function of the stripping time, t_a, at a potential $E_a = 150$ mV for a bar which had been coated with copper for 30 s at various cathodic currents. The temperature was 323 K and the solution flow rate 0.84 m s^{-1} during both copper dissolution and copper deposition.

the shape of the I_a/t_a curve was evident; splitting was found every time at 303 K, sometimes at 323 K depending on i and v, and never at 343 K. The change in shape of the I_a/t_a curves may be caused by the formation of passive films. Lowering the temperature facilitates the onset of passivity [7]. This agrees with the dependence on temperature of the splitting up of the I_a/t_a curve.

3.4. *Effect of electrochemical conditions during anodic stripping on the* Q_a/Q_c *ratio*

Petit [8] has found that the number of electrons, n_a, used for dissolution of one copper atom depends on the anodic stripping potential and lies between 1 and 2 for cupric sulphate solutions, owing to the formation of both Cu(II) and Cu(I).

Assuming two electrons for deposition of one copper atom from cupric sulphate solution, the ratio Q_a/Q_c is a measure of n_a. Figure 3 shows Q_a/Q_c as a function

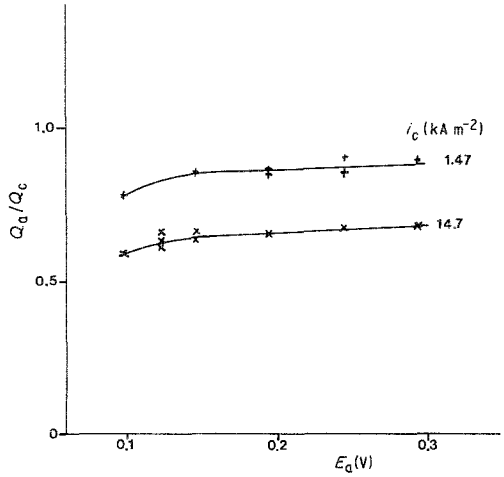

Fig. 3. The ratio Q_a/Q_c as a function of the potential, E_a, during anodic stripping of a bar which had been coated with copper for 30 s at two different current densities. During both copper dissolution and copper deposition the temperature was 323 K and the solution flow rate 0.84 m s^{-1}.

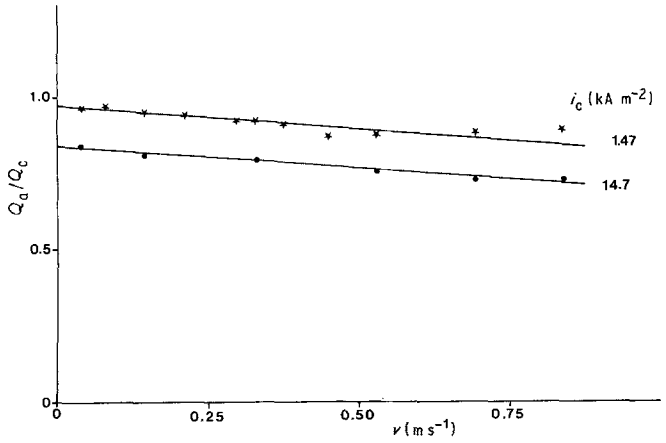

Fig. 4. The ratio Q_a/Q_c as a function of the rate of solution flow during the anodic stripping of a copper layer which had been deposited for 30 s at two different current densities, solution flow rate of 0.84 m s^{-1} and at 323 K.

of the potential, E_a, of the working electrode during its anodic stripping at 323 K and $v = 0.84\,\mathrm{m\,s^{-1}}$. The copper coating of the working electrode was formed at two different current densities. The same electrolytic conditions, except the potential, were used during the anodic stripping and the cathodic deposition. From Fig. 3 it follows that Q_a/Q_c increases slightly and approaches a limiting value. The same result was obtained for experiments at 333 and 343 K.

The effect of the rate of solution flow during anodic dissolution of a copper coating at 0.25 V on Q_a/Q_c is shown in Fig. 4. The copper coating was formed at 323 K, a solution flow rate of 0.84 m s^{-1} and at two different current densities during a polarization time of 30 s. Figure 4 shows that Q_a/Q_c decreases linearly with increasing rate of solution flow during copper dissolution. It is likely that this decrease in Q_a/Q_c is caused by the increasing rate of diffusion of Cu(I) from the electrode surface to the bulk of solution, so that further electrochemical oxidation to Cu(II) is prevented. In the absence of forced convection, diffusion of Cu(I) to the bulk of the solution will be negligible. Taking into account the relatively slight effect of the potential during anodic stripping at potentials higher than about 0.2 V (Fig. 3) and the results of Petit [8], it can be concluded that Q_a, in the absence of forced convection and at potentials higher than 0.2 V, denoted by Q_a^*, is equal to Q_a for $n_a = 2$ electrons/copper atom. The current efficiency, η_{Cu}, for the copper deposition is given by $\eta_{Cu} = Q_a^*/Q_c$.

Because of the effects of the solution flow and the potential, E_a, on Q_a, the anodic stripping was generally carried out at a potential of 0.2 V and in the absence of forced convection.

3.5. *Current efficiency for copper deposition*

It has been found that the current efficiency η_{Cu} of copper does not depend on the sequence of the cathodic current densities during a series of experiments. Experiments with a constant time (30 s) of cathodic polarization give the same copper current efficiency as experiments with a constant quantity of charge (750 C) used during copper deposition. It was found that the potential of the working electrode was constant during the polarization time of 30 s at $v = 0.84\,\mathrm{m\,s^{-1}}$ and at $i_c < 9\,\mathrm{kA\,m^{-2}}$, and that it decreased at a decreasing rate with increasing time of polarization at $i_c > 9\,\mathrm{kA\,m^{-2}}$. Figure 5 shows η_{Cu} as a function of current density at various rates of flow. From this figure it follows that for $i_c < 3\,\mathrm{kA\,m^{-2}}$ the copper current efficiency is almost 1 and at higher current densities this efficiency declines with increasing i_c. This decline depends on the rate of solution flow.

From potential and ohmic potential drop measurements it follows that, for the experiments in Fig. 5, the potential during copper deposition at $i_c > 9\,\mathrm{kA\,m^{-2}}$ is negative versus the RHE and decreases very sharply with increasing i_c; for instance, $E = -0.24$, -0.42 and -0.65 V for $i_c = 8.8$, 11.8 and 14.7 kA m^{-2}, respectively.

The effect of the rate of solution flow on η_{Cu} at

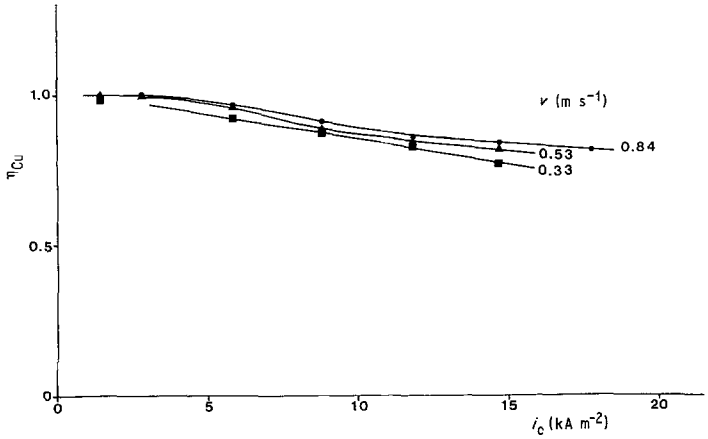

Fig. 5. Copper current efficiency as a function of current density, i_c, during copper deposition at various solution flow rates and at 323 K.

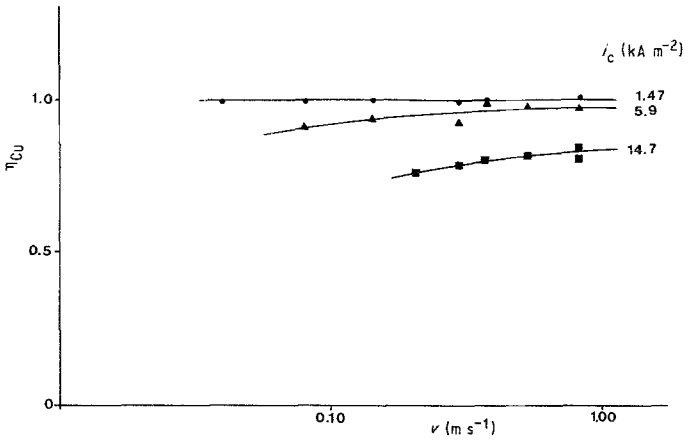

Fig. 6. Copper current efficiency as a function of solution flow rate during copper deposition at various current densities and 323 K.

various i_c is given in Fig. 6. This figure shows that η_{Cu} increases with increasing v.

Figure 7 shows the effect of the temperature at various i_c on η_{Cu}. From this figure it follows that i_c determines the effect of the temperature on η_{Cu} to different degrees.

3.6. *Mass transfer of Cu(II) in the absence of hydrogen evolution*

The E/I_c curves for the dilute cupric sulphate–sulphuric acid solution are useful in determining a limiting current, $I_{L,Cu}$, for copper deposition. No limiting current region has been found for the concentrated solution. For the dilute solution, the contribution of migration to the mass transfer of Cu(II) is negligible, owing to an excess of supporting electrolyte. Using the relation $I_{L,Cu(II)} = nFA_e k_{Cu(II)} c^s_{Cu(II)}$ and substituting $n = 2$ for the reaction Cu(II) + $2e^- \rightarrow$ Cu, F = 96500 C mol^{-1}, $A_e = 17 \times 10^{-4}$ m^2 and $c^s_{Cu(II)} = 20$ mol m^{-3}, the mass transfer coefficient $k_{f,Cu(II)}$ on a circumference-averaged basis can be calculated from the experimental $I_{L,Cu(II)}$. In Fig. 8 $k_{f,Cu(II)}$ is plotted vs v for forced convection at 323 K. The results at 0.05 m s^{-1} < v < 1.0 m s^{-1} can be given by $k_{f,Cu(II)} = [2.5 + 13.5v] \times 10^{-5}$ m s^{-1}.

Plotting the results of Fig. 8 on a double logarithmic scale, it has been found that the slope of the log $k_{f,Cu(II)}$/log v curve is 0.73 at v from 0.30 to 1.0 m s^{-1}.

It has been found that the effect of temperature on $k_{f,Cu(II)}$ at 1.0 m s^{-1} is given by $k_{f,Cu(II)}(T) = 9.14 \times 10^{-5} \exp[-2.0 \times 10^3(1/T - 1/298)]$ m s^{-1}.

3.7. *Mass transfer of Cu(II) with evolution of hydrogen bubbles*

The current efficiency for copper deposition from the dilute cupric sulphate–sulphuric acid solution has been determined as a function of current density and solution flow rate in the current range where hydrogen evolution occurs at a high rate.

Assuming that hydrogen is the only by-product, then $i_H = (1 - \eta_{Cu})I_c/A_e$. Analogously to the calculation of $k_{f,Cu(II)}$ (3.6), $k_{Cu(II)}$ was calculated as a function of i_H. The result is given in Fig. 9. From this figure it is deduced that, for the dilute solution, the mass transfer coefficient on a circumference-averaged basis, $k_{Cu(II)} = (3.2 + 9.0v + 1.3i_H) \times 10^{-5}$ m s^{-1}, where v is in m s^{-1} and i_H in kA m^{-2}. A similar relation has been found for a hydrogen-evolving electrode in alkaline solution [9].

4. Discussion

4.1. *Electrode reactions*

The electrodeposition of copper occurs according to a two-step mechanism [7], namely

$$\text{step 1: Cu(II)} + e^- \longrightarrow \text{Cu(I)}$$

$$\text{step 2: Cu(I)} + e^- \longrightarrow \text{Cu}$$

It is well known that Cu(I) can be formed as an intermediate species at the cathode surface during

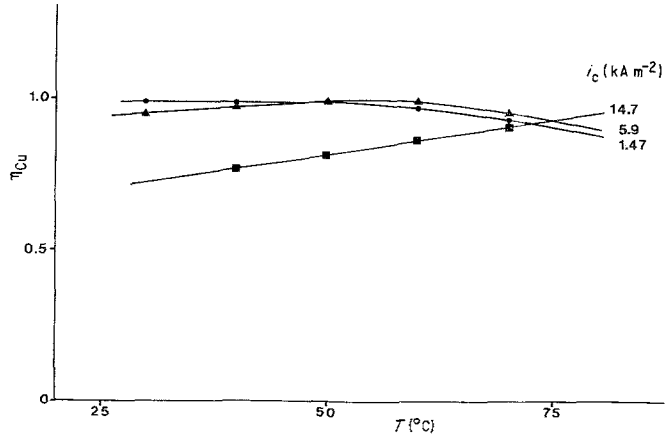

Fig. 7. Copper current efficiency as a function of temperature during copper deposition at various current densities and at a solution flow rate of 0.84 m s^{-1}.

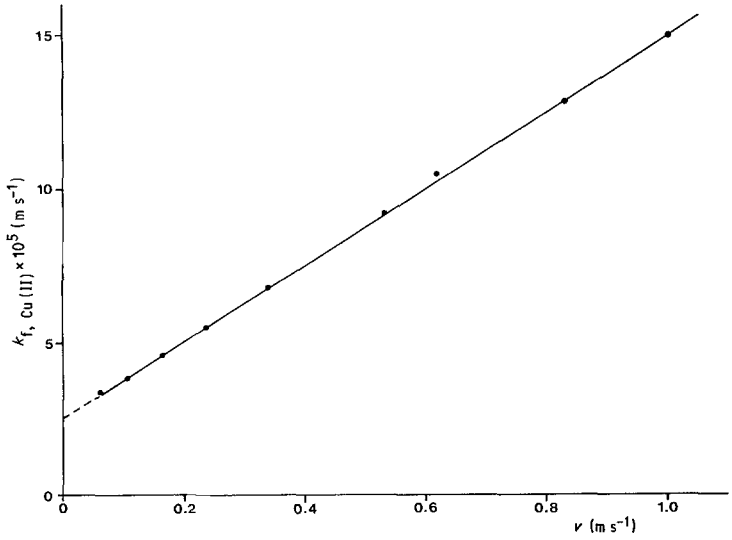

Fig. 8. Diffusion mass transfer coefficient for Cu(II) in a dilute cupric sulphate–sulphuric acid solution as a function of the rate of solution flow at 323 K.

copper deposition from an acid cupric sulphate solution [10].

Mattson and Bockris [11] have found that step 1 is rate determining and step 2 is in equilibrium during copper deposition from a cupric sulphate–sulphuric acid solution. For this case it can be shown that at potentials $E < 0$ V, the Cu(I) concentration at the electrode surface as well as the rate of diffusion of Cu(I) to the bulk of solution are extremely low.

Despite this result, Levum *et al.* [12] have found that the rate of copper deposition on a flat stainless-steel cathode with complicated solution flow conditions decreases substantially with increasing *Re* at constant cathodic current density and at very high *Re*; for instance, at 2.3 kA m^{-2} a decline of about 50% was obtained for an increase in *Re* from 10^4 to 2×10^4. They assume the formation of Cu(I) ions which are carried away by the solution flow from the electrode and so do not participate in the reaction Cu(I) + e^- → Cu.

In this study it has been found that the dependence of η_{Cu} on v differs completely from that reported by Levum *et al.* [12]. This discrepancy is probably caused by a difference in *Re* and the geometry of the cell and working electrode. Since η_{Cu} increases with increasing v (Figs 5 and 6), it is likely that, under our experimental conditions, hydrogen is the main by-product and that the current efficiency loss due to diffusion of cuprous ions to the bulk of solution is negligible.

4.2. *Mass transfer of Cu(II) in the absence of hydrogen evolution*

From Section 3.6 it follows that the slope of the log $k_{f,Cu(II)}$/log v curve at solution flow rates from 0.30 m s^{-1} to 1.0 m s^{-1} (*Re* from 987 to 3290) is equal to 0.73. This slope is much higher than that generally given. The literature values vary between 0.40 and 0.56, depending on *Re* [13, 14]. This difference may be caused by differences in cell design. In particular, the dimensions of the slots in the inner Perspex cylinder and the relatively short distance between the entrance of the working-electrode compartment and the working-cylinder electrode will affect the hydrodynamic behaviour of the solution flow around the working-cylinder electrode.

Assuming that $k_{f,Cu(II)}$ is proportional to $(D_{Cu(II)})^{2/3}$ $v^{-1/6}$, from $k_{f,Cu(II)}$ for the dilute solution, that for the concentrated cupric solution can be calculated. The result is given by $k_{f,Cu(II)} = [2.15 + 11.6v] \times 10^{-5}$ m s^{-1}. A similar correlation, namely $Sh = (0.35 + 0.56Re^{0.52})Sc^{0.33}$, can be deduced from the McAdams correlation [20] for heat transfer from a cylinder to a solution, directed perpendicularly onto the axis of the cylinder. Since $Re = v_c d_c/\nu$ and $Sh = kd_c/D$, it is clear that the dependence of k on the solution flow rate, v_c, differs in both correlations. This difference may be caused by the cell geometry.

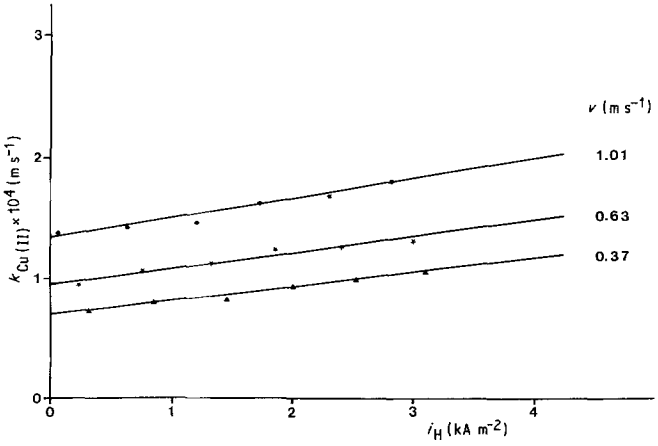

Fig. 9. Diffusion mass transfer coefficient for Cu(II) in a dilute cupric sulphate–sulphuric acid solution as a function of the current density, i_H, for hydrogen evolution at 323 K and various solution flow rates.

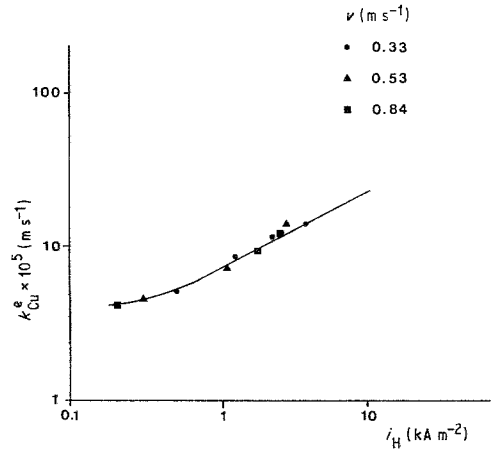

Fig. 10. The electrochemical rate constant for copper deposition from the concentrated cupric sulphate solution as a function of current density i_H at 323 K and at various solution flow rates.

4.3. *Rate-determining step for copper deposition*

It is assumed that the current efficiency loss, $1 - \eta_{Cu}$, is completely attributed to hydrogen evolution. To answer the question whether, for the concentrated cupric solution, the Cu(II) concentration at the cathode surface, $c^{\sigma}_{Cu(II)}$, is practically equal to zero in the current density region where hydrogen is also evolved, we need $k_{Cu(II)}$. From $k_{Cu(II)}$ for the dilute solution and assuming that $k_{Cu(II)}$ is proportional to $(D_{Cu(II)})^{2/3} v^{-1/6}$, it can be shown that $k_{Cu(II)} = (2.75 + 7.7v + 1.1i_H) \times 10^{-5}$ m s^{-1} for the concentrated cupric solution where i_H indicates the current density for H_2 evolution.

The limiting current for copper deposition has been calculated as a function of i_H and v, using the relation

$$I_{L,Cu(II)} = 2FA_e k_{Cu(II)} c^{s}_{Cu(II)} (1 + t_{Cu(II)})$$

where $t_{Cu(II)}$ is half of $t_{Cu(II)}$ for the bulk of the solution (Table 1). The calculation shows that, under the conditions in Figs 5 and 6, the limiting current density, $I_{L,Cu}$, is at least a factor 2.0 higher than the current density.

Consequently, for the concentrated cupric solution, the current efficiency for copper deposition, even at high current densities, is determined by both the mass transfer of cupric ions and the kinetic parameters of the electrochemical copper deposition.

4.4. *Current efficiency for copper deposition*

From the electrochemical reaction kinetics and diffusion theory, it can be deduced that the rate of copper deposition at $E - E_{r,Cu} < -60$ mV for the reaction Cu(II) + $2e^- \rightarrow$ Cu is

$$i_{Cu} = 2Fc^{\sigma}_{Cu(II)} k^{e}_{Cu(II)} \quad (1)$$

where

$$c^{\sigma}_{Cu(II)} = \frac{i_{L,Cu} - i_{Cu}}{2F(1 + t_{Cu(II)})k_{Cu(II)}} \quad (2)$$

and

$$i_{L,Cu} = 2F(1 + t_{Cu(II)})k_{Cu(II)} c^{s}_{Cu(II)} \quad (3)$$

From Equations 1–3 inclusive, it follows that

$$k^{e}_{Cu(II)} = \frac{i_{Cu}(1 + t_{Cu(II)})k_{Cu(II)}}{2F(1 + t_{Cu(II)})k_{Cu(II)} c^{s}_{Cu(II)} - i_{Cu}} \quad (4)$$

For the reaction $2H^+ + 2e^- \rightarrow H_2$, and neglecting concentration polarization, it can be deduced that at $E - E_{r,H} < -60$ mV

$$i_H = Fk^{e}_{H} c^{s}_{H+} \quad (5)$$

As D_{H+} is about a factor of 13 higher than $D_{Cu(II)}$ [15] it is evident that $c^{\sigma}_{H+} \simeq c^{s}_{H+}$ in the i_H range for practical conditions in the high-rate copper deposition process. In general it can be stated that relation 5 is useful from current densities i_H around 10^{-2} kA m^{-2} [16].

Though the potential and the mass transfer coefficient differ around the bar, the relations for i_{Cu} and i_H are applied to derive a practical correlation for the current efficiency of copper deposition. It must be noted that both the electrochemical constant and the mass transfer coefficient are average for the circumference of the round bar. Substituting $k_{Cu(II)}$ for the concentrated solution (4.2), $t_{Cu(II)} = 0.08$ (half of $t_{Cu(II)}$ for the concentrated solution), $i_{Cu} = I_c \eta_{Cu}/A_e$ where η_{Cu} is obtained from Fig. 5 into (4), $k^{e}_{Cu(II)}$ is determined

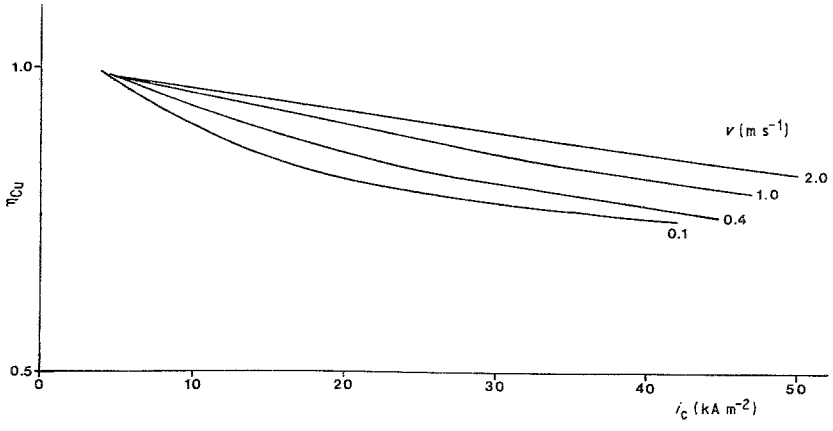

Fig. 11. Calculated copper current efficiency as a function of i_c for a 1 M H_2SO_4 + 1.5 M $CuSO_4$ solution at 323 K and various solution flow rates.

as a function of i_H where $i_H = (I_c - I_{Cu})/A_e$ for various solution flow rates. The result is given in Fig. 10.

From this figure it follows also that, in the current density range from 0.5 to 3 kA m^{-2}, $k^e_{Cu(II)} \sim 7.6 \times 10^{-5}\, i_H^{0.56}$ m s^{-1} where i_H is given in kA m^{-2}.

The current efficiency for copper deposition is defined by

$$\eta_{Cu} = i_{Cu}/(i_{Cu} + i_H) \quad (6)$$

where

$$i_{Cu} + i_H = i_c \quad (7)$$

It has been found that it is not possible to present a simple correlation for η_{Cu} as a function of various parameters. A set of relations has been obtained to calculate η_{Cu} using a computer.

This set of relations consists of the one for $k_{Cu(II)}$ (4.3), that for $k^e_{Cu(II)}$ as a function of i_H (4.4), and the relations 4, 6 and 7. The current efficiency η_{Cu} can be calculated as a function of the flow rate of solution, current density, temperature and concentration of cupric sulphate where kinematic viscosity of solution, diffusion coefficient for Cu(II) and transference number for Cu(II) are taken into account. For example, η_{Cu} is given as a function of i_c in Fig. 11 for a 1 M H_2SO_4 + 1.5 M $CuSO_4$ solution at 323 K and various rates of solution flow. This figure clearly shows the dependence of η_{Cu} on the rate of flow and the current density for a fixed composition of the copper bath.

References

[1] W. H. Safranek, in 'Modern Electroplating' (edited by F. A. Lowenheim), 3rd edn, John Wiley, New York (1974) p. 183.
[2] Private communication (1984).
[3] G. Wranglen and O. Nilsson, *Electrochim. Acta* 7 (1962) 121.
[4] J. Newman, *Ind. Engng Chem. Fund.* **5** (1966) 525.
[5] E. Ravoo, thesis, Twente (1971).
[6] W. H. McAdams, in 'Heat Transmission', Chemical Engineering Series (edited by S. D. Kirkpatrick), 3rd edn, McGraw-Hill Book Company, New York (1954) p. 266.
[7] U. Bertocci and D. R. Turner, 'Encyclopedia of Electrochemistry of the Elements', (edited by A. J. Bard), Marcel Dekker, New York, (1974) Vol. II, p. 455.
[8] M-C. Petit, *Electrochem. Acta* **10** (1965) 291.
[9] L. J. J. Janssen and E. Barendrecht, Dechema-Monographien Band 98, Verlag Chemie (1985) 463.
[10] L. M. Nekrasov and N. P. Berezina, *Dokl. Akad. Nauk. SSSR* **142** (1962) 855.
[11] E. Mattson and J. O'M. Bockris, *Trans. Faraday Soc.* **55** (1959) 1586.
[12] M. L. Levum, I. V. Tsvetkov and A. D. Davydon, *Soviet Electrochem.* **18** (1982) 1417.
[13] A. Tvarusko, *J. Electrochem. Soc.* **123** (1976) 489.
[14] P. Grassman, N. Ibl and J. Trüb, *Chemie-Ing.-Techn.* **33** (1961) 529.
[15] I. M. Kolthoff and J. J. Lingane, 'Polarography', Interscience, New York (1952) Vol. 1, p. 52.
[16] A. J. Appleby, M. Chemila, H. Kita and G. Bronoël, 'Encyclopedia of Electrochemistry of the Elements', (edited by A. J. Bard), Marcel Dekker, New York, (1982) Vol. IX, Part A, p. 459.
[17] G. W. Tindall and S. Bruckenstein, *Analyt. Chem.* **40** (1968) 1402.
[18] F. Fenwick, *J. Am. Chem. Soc.* **48** (1926) 860.
[19] W. M. Latimer, 'The Oxidation States of the Elements and their Potentials in Aqueous Solution', 2nd edn, Prentice-Hall, Englewood Cliffs, N.J. (1956).
[20] J. P. Holman, 'Heat Transfer', 4th edn, McGraw-Hill Kogakusha, Tokyo (1976).